CHEMISTRY OF MATERIALS

Article

pubs.acs.org/cm

From Exothermic to Endothermic Dehydrogenation – Interaction of Monoammoniate of Magnesium Amidoborane and Metal Hydrides

Yong Shen Chua,[†] Wen Li,[†,‡] Guotao Wu,[†] Zhitao Xiong,[†] and Ping Chen*[,†]

[†]Dalian Institute of Chemical Physics, Dalian 116023, People's Republic of China

[‡]Department of Physics, National University of Singapore, Singapore 117542

Supporting Information

ABSTRACT: Metal amidoborane ammoniate such as $Mg(NH_2BH_3)_2{\cdot}NH_3$ and $Ca(NH_2BH_3)_2{\cdot}nNH_3$ with n = 1, 2, release NH_3 predominantly and endothermically at low temperatures in an open-system. However, a strong exothermic reaction occurs when these ammoniates were dehydrogenated in a closed-system, where the adducted NH_3 take part in the reaction. Our approach in tailoring the thermodynamic properties of $Mg(NH_2BH_3)_2{\cdot}NH_3$, by replacing its adducted NH_3 with amide was successful, yielding a composite consisting of bimetallic amidoborane and $Mg(NH_2)_2$. Crystal structures of bimetallic amidoboranes, i.e., $Na_2Mg(NH_2BH_3)_4$ and $K_2Mg(NH_2BH_3)_4$ were identified and solved. Significant improvement in the dehydrogenation thermodynamic was observed in the composite system as compared to the pristine $Mg(NH_2BH_3)_2{\cdot}NH_3$, i.e., the dehydrogenation enthalpies were altered from an exothermic to an endothermic one. In addition, the detection of bimetallic amidoboranes in the composites urges detailed investigation on pristine bimetallic amidoborane, to which later we found that $Na_2Mg(NH_2BH_3)_4$ also dehydrogenated endothermically at the identical temperature range (ca. 150−170 °C) with that of composite systems. Similar activation barriers were observed in $Na_2Mg(NH_2BH_3)_4$ and composite systems, suggesting that metal hydride mediation may be the internal barrier that dominates the kinetic barrier of the composite system. First-principles calculations also showed that the thermodynamic stability of metal amidoborane (MNH_2BH_3, MAB) increases with decreasing Pauling electronegativity of the metal. Based on the calculated results, a reactant stabilization approach was proposed, which suggests that forming a stable reactant is an effective way of reducing the exothermicity of the dehydrogenation of metal amidoborane.

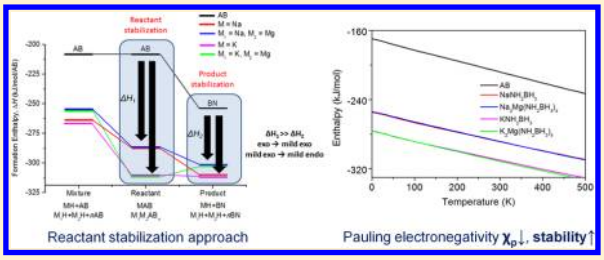

KEYWORDS: *hydrogen storage, amidoborane, endothermic, dehydrogenation*

INTRODUCTION

Burdened by the increasing oil price, scarce energy resources, and the dawning realization of the environmental crisis, a flurry of meaningful research has been devoted into clean and sustainable energy. Hydrogen has been recognized as a potential alternative energy carrier because it is clean, ubiquitous, and possesses high energy density of 120−142 MJ/kg. It can be used either on-board or off-board. For the on-board application, a safe and efficient hydrogen storage media is needed. Today, hydrogen storage is still a key technological challenge in the wide implementation of hydrogen fuel cell vehicles.

Having a hydrogen capacity of 19.6 wt % and good stability under ambient condition, ammonia borane, NH_3BH_3 (AB for short), has received considerable attention as a potential hydrogen storage material.[1,2] However, its dehydrogenation suffers from slow kinetic, sample foaming, and contamination of volatile byproducts. Improvements in the dehydrogenation kinetics and thermodynamics of AB have been achieved by using various approaches, including compositional alteration, catalytic modification, and nanoconfinement.[2−4] Particularly, compositional alteration of AB by using metal hydride to induce formation of a new compound, which demonstrates significant thermodynamic improvement with reduced dehydrogenation temperature.[5] Such improvements were achieved as a result of the substantial changes in the bonding chemistry of AB after substituting its protonic H with a more electropositive metal (via acid−base reaction) to form metal amidoboranes, $M-(NH_2BH_3)_m$ (M = Li, Na, K, Ca, Sr, Y, etc., m is the valence of M) or bimetallic amidoboranes, $M_1M_2(NH_2BH_3)_{m+n}$ (M_1M_2 = LiNa, NaMg, and Na_2Mg, m and n are the valence of M_1 and M_2).[5−14] The explicit dehydrogenation mechanisms especially those responsible for the improved dehydrogenation properties of metal amidoborane were reported based on both theoretical calculations and experiments.[15−22] In addition to these conventional modification approaches via metal hydride addition, interactions of AB and metal amides (NH_2^-) and imides (NH^{2-}) were also reported recently. Owing to the stronger Lewis base of NH_2^- or NH^{2-} than $NH_2BH_3^-$ in AB, proton H^+ transfer from AB to stronger Lewis base group occurs, giving rise to metal amidoborane ammoniates, for instance $M-(NH_2BH_3)_m{\cdot}nNH_3$,

Received: May 30, 2012
Revised: August 16, 2012
Published: August 21, 2012

 © 2012 American Chemical Society dx.doi.org/10.1021/cm301662q | *Chem. Mater.* 2012, 24, 3574−3581

(M = Li, Mg, Ca).[23−26] These ammoniates decompose at relatively low temperatures with stoichiometric conversion of NH_3 to H_2 when heated in a closed-system, showing further improvement in hydrogen storage properties compared to metal amidoboranes.

Although the thermodynamics and kinetics of dehydrogenation have been improved via the formation of metal amidoboranes ammoniates, those chemical hydrides are still unfavorable for hydrogen storage due to the exothermic nature of dehydrogenation, giving rise to the formation of the thermodynamically stable B−N product. Due to the fact that endothermicity is a prerequisite for achieving an energy efficient regeneration/reversible process, further thermodynamic alteration/improvement on existing potential materials is thus indispensable. In particular, $Mg(NH_2BH_3)_2{\cdot}NH_3$ is of interest due to its high hydrogen content (12.8 wt %) and strong NH_3 coordination with Mg^{2+}.[26] $Mg(NH_2BH_3)_2{\cdot}NH_3$ decomposes to H_2 at ca. 50 °C with minor coproduction of NH_3. When heated in a closed-system, it releases ca. 6 equiv of H_2 (or 11.8 wt %) with the absence of NH_3, forming $[MgB_2N_3H]$. Thermodynamic investigation on metal amidoborane ammoniates clearly showed a strong exothermic hydrogen release occurred in a closed-system at low temperatures followed by mild dehydrogenation process (see Supporting Information, Figure S1). It was also evidenced by the recent mechanistic investigation on the dehydrogenation of calcium amidoborane ammoniate that the adducted NH_3 actually takes part in the first dehydrogenation step, reacting a $H^{\delta+}$ (NH_3) with a $H^{\delta-}$ (BH_3) and concurrently forming B−N bond − the contributing factor for the exothermic reaction.[27−29] Investigations on thermal decomposition of calcium amidoborane ammine complex in hydrocarbon-soluble model by Harder and co-workers[30] also corroborate this result. In fact, in their study they proposed that β-H elimination (or metal hydride mediated) followed by deprotonation of NH_3 is more likely to occur in the dehydrogenation process. In this case, NH_3 indeed plays a vital role in tuning the thermodynamic properties of metal amidoboranes. The interaction of metal hydride and NH_3 is known to be an exothermic process due to the formation of thermodynamically stable metal amide, with the driving force involving Coulombic attractions of oppositely charged atoms ($H^{\delta+}$ and $H^{\delta-}$, M^+ and N^-) (see reaction 1).[31] However, different from NH_3, it was demonstrated that the interaction of lithium hydride and lithium amide is an endothermic process, which is mainly due to the formation of lithium imide − a thermodynamically less stable product than the starting reactants (reaction 2).[32] Herein, in order to avoid the strong exothermic reaction directed from the interaction of NH_3 with amidoborane, we tentatively introduce metal hydrides, i.e. sodium hydride, NaH, or potassium hydride, KH, to react with the adducted NH_3, with the hypothesis of the formation of a composite consisting of amides (sodium amide, $NaNH_2$, or potassium amide, KNH_2) and metal amidoborane via reaction 3 based on amide−hydride interaction approach and subsequently investigate the interaction between these two components.

$$NH_3 + MH_n \rightarrow M(NH_2)_n + H_2 \quad (1)$$

$$LiNH_2 + LiH \rightarrow Li_2NH + H_2 \quad (2)$$

$$Mg(NH_2BH_3)_2{\cdot}NH_3 + MH \rightarrow Mg(NH_2BH_3)_2 + MNH_2 + H_2,\ M = K, Na \quad (3)$$

Beyond our expectation, interaction of $Mg(NH_2BH_3)_2{\cdot}NH_3$ and KH or NaH did not result in the formation of $[Mg(NH_2BH_3)_2{+}KNH_2]$ or $[Mg(NH_2BH_3)_2{+}NaNH_2]$ composite. Instead, $[K_2Mg(NH_2BH_3)_4{+}Mg(NH_2)_2]$ and $[Na_2Mg(NH_2BH_3)_4{+}Mg(NH_2)_2]$ composites were formed with the detection of new structures, $K_2Mg(NH_2BH_3)_4$ and $Na_2Mg(NH_2BH_3)_4$. More importantly, these composites dehydrogenate endothermically at ca. 158 and 153 °C. To the best of our knowledge, this is the first example on the investigation of metal amidoborane with metal amide and is the first few reported AB-based material which undergoes endothermic dehydrogenation.

EXPERIMENTAL SECTION

$Mg(NH_2BH_3)_2{\cdot}NH_3$ was prepared as described in ref 26. Mixtures of $Mg(NH_2BH_3)_2{\cdot}NH_3$ and KH (30−35% w/w in mineral oil, Alfa Aesar−prewashed with cyclohexane) or NaH (95%, Sigma Aldrich) in the molar ratio of 1:1 was milled on a Retsch PM400 at 200 rpm for 10 h. All the materials handlings were performed inside a Mbraun glovebox that was filled with purified argon. $Na_2Mg(NH_2BH_3)_4$ was synthesized via a liquid state approach. A mixture of $Mg(NH_2)_2$ (self-prepared, >95% purity), NaH, and AB with the molar ratio of 1/2/4 was added in an autoclave, and pressure increase was monitored with time. Approximately 0.7 equiv of gaseous product was released per AB. Mass spectrometer (MS) analysis on the gaseous product formed in the reaction evidenced the formation of H_2 and NH_3, suggesting an interaction between $Mg(NH_2)_2$−2AB and NaH−AB. Two phases were obtained. One is soluble in solvent THF and another forms a precipitate. XRD and FTIR results (see Figures S2 and S4) show that powder obtained from supernatant and precipitate are of two different phases, with the XRD pattern of the precipitate matches with $Na_2Mg(NH_2BH_3)_4$ reported by Wu et al.[12] (see Figure S13). DSC and volumetric release measurement on $Na_2Mg(NH_2BH_3)_4$ were also illustrated in Figure S7.

Structure identifications were carried out on a PANalytical X'pert diffractometer with Cu Kα radiation (40 kV, 40 mA). The obtained data were indexed using TREOR or DICVOL programs. Candidate structures were obtained by performing combined direct space simulated annealing and first principle calculations. Rietveld structural refinement analyses were performed using the GSAS.[33] FTIR measurements were conducted on a Varian 3100 unit in DRIFT mode. *Thermal desorption behavior* of the postmilled samples were investigated by using a homemade temperature-programmed desorption coupled with a mass spectrometer (TPD−MS). Thermogravimetry and differential scanning calorimetry (DSC) measurements were performed on a Netsch 449C TG/DSC unit. A dynamic flow mode was employed with purified argon as a carrier gas, and the heating rate was set at 2 °C/min (open-system). C80 (Setaram) on the other hand was used for closed-system calorimetric measurement. The quantitative measurements of gas evolution from samples (i.e., volumetric release) were performed on a homemade Sievert type reactor. *NH_3 concentration* was determined by using a conductivity meter (Thermo Scientific) with the accuracy of 0.1 μS/cm. 100 mL of (0.0006 M) diluted sulfuric acid (H_2SO_4) solution was prepared. At the end of quantitative measurement (i.e., volumetric dehydrogenation conducted in the Sievert type reactor), gaseous product accumulated in the reactor was bubbled in the diluted H_2SO_4 solution. The change in conductivity of the solution reflects the amount of NH_3 trapped by the solution and correlates to NH_3 coproduced in the dehydrogenation.

Theoretical Calculation. For the first-principle calculations based on the density function theory (DFT) and the pseudopotential plane wave method, we adopted the projector augmented wave (PAW) pseudopotentials[34] as implemented in the Vienna ab initio simulation package (VASP).[35,36] The generalized gradient approximation (GGA-PW91) was used to treat the electronic exchange-correlation energy. Full ionic relaxation and volumetric relaxation were conducted on the geometry optimized candidate structure until self-consistency was

dx.doi.org/10.1021/cm301662q | Chem. Mater. 2012, 24, 3574−3581

achieved within a tolerance of a total energy of 0.01 meV and atomic forces of 0.01 eV/Å. Phonon density of state and reaction enthalpy were calculated using the direct method,[37,38] which was implemented in the Phonopy program[39] combined with VASP code. Hellmann–Feynman forces on all atoms in the supercell were calculated with the displacements of 0.03 Å for each symmetrically nonequivalent atom from their respective equilibrium positions in three independent directions. A complete force-constant matrix was obtained, and the phonon frequencies (ω) were then calculated by a diagonalization of the dynamical matrix. A 2 × 2 × 2 supercell of solid AB, a 2 × 2 × 1 supercell of crystal KAB, and a 1 × 2 × 2 supercell of NaAB and unit cells of Na_2MgAB_4 and K_2MgAB_4 were employed for the phonon calculations. The PAW GGA potential, cutoff energies, and the self-consistent field convergence parameters were chosen to be the same as for the static energy calculations described above, while atomic forces were converged to be lower than 0.001 eV/Å.

RESULTS AND DISCUSSION

The mixtures of $Mg(NH_2BH_3)_2{\cdot}NH_3$ and KH (or NaH) in the molar ratio of 1:1 were ball milled under Ar atmosphere at 200 rpm for 10 h, and ca. 1 equiv of hydrogen was released with a detectable amount of NH_3 (ca. 3%). Because neither $Mg(NH_2BH_3)_2{\cdot}NH_3$ nor KH (or NaH) decomposes under ball milling, the hydrogen evolved should be due to the occurrence of the interaction between KH (or NaH) and the adducted NH_3 (similar to the reaction 1), agreeing with our hypothesis described in reaction 3. XRD powder diffraction measurements on the postmilled samples (Figure 1) evidenced

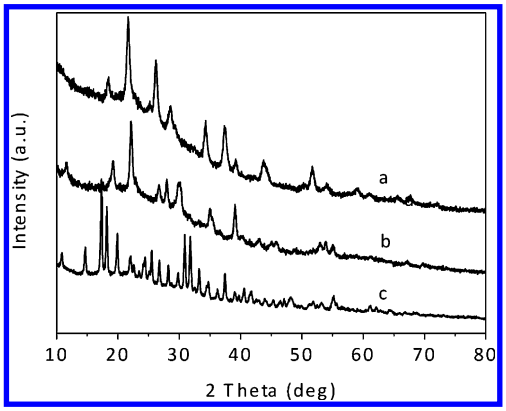

Figure 1. XRD patterns of (a) the postmilled $Mg(NH_2BH_3)_2{\cdot}NH_3$ and KH sample, (b) postmilled $Mg(NH_2BH_3)_2{\cdot}NH_3$ and NaH sample, and (c) $Mg(NH_2BH_3)_2{\cdot}NH_3$.

the absence of $Mg(NH_2BH_3)_2{\cdot}NH_3$ and KH (or NaH) and the development of a new set of diffraction peaks which do not match any of the known compounds in the database. Instead, the XRD pattern of the postmilled $Mg(NH_2BH_3)_2{\cdot}NH_3$ and NaH sample matched fairly well with the diffraction pattern of $Na_2Mg(NH_2BH_3)_4$, which was reported recently by Wu et al.[12] Along with the detection of $Na_2Mg(NH_2BH_3)_4$, one can reasonably deduce that the metal cation in hydride (MH) is likely to undergo cation exchange and NH_3 abstraction with $Mg(NH_2BH_3)_2{\cdot}NH_3$ yielding bimetallic amidoborane and magnesium amide (reaction 4) rather than simply abstracting an adducted NH_3 by NaH (or KH) to form $NaNH_2$ (or KNH_2) (reaction 1).

$$2Mg(NH_2BH_3)_2{\cdot}NH_3 + 2MH \rightarrow M_2Mg(NH_2BH_3)_4 + Mg(NH_2)_2 + 2H_2,\ M = Na, K \quad (4)$$

Because of the facile deformation of $Mg(NH_2)_2$ to an amorphous state under ball milling conditions, both XRD and FTIR data (see Figure 2, broadened peaks overlapping with

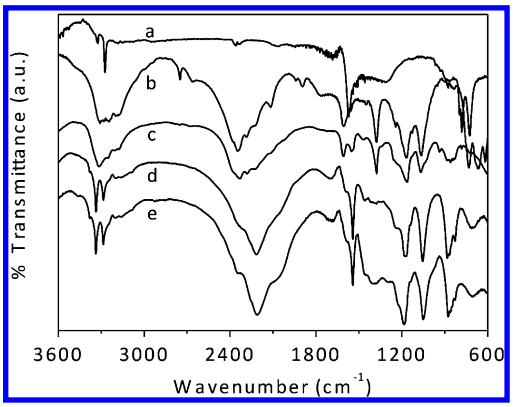

Figure 2. FTIR spectra of (a) $Mg(NH_2)_2$, (b) AB, (c) $Mg(NH_2BH_3)_2{\cdot}NH_3$, (d) postmilled $Mg(NH_2BH_3)_2{\cdot}NH_3$+KH sample, and (e) the postmilled $Mg(NH_2BH_3)_2{\cdot}NH_3$+NaH sample.

other N–H stretching) could not give distinct evidence of its existence.[40] In an independent experiment, we ball milled $Na_2Mg(NH_2BH_3)_4$ and $Mg(NH_2)_2$ in a molar ratio of 1:1 for 5 h at 150 rpm and found that the postmilled sample exhibits identical XRD and FTIR features as that of the postmilled $Mg(NH_2BH_3)_2{\cdot}NH_3$+NaH sample (see Supporting Information, Figures S2, S3, and S4). Because of the prolonged ball milling process, significant peak broadening was observed in the XRD patterns of the postmilled samples. Furthermore, it was evidenced by ^{11}B magic angle spinning (MAS) NMR (Figure S5) that the postmilled $Mg(NH_2BH_3)_2{\cdot}NH_3$+NaH sample exhibited an identical boron chemical shift (−24 ppm) to that of $Na_2Mg(NH_2BH_3)_4$ and the postmilled $Na_2Mg(NH_2BH_3)_4$+$Mg(NH_2)_2$ (1:1) samples, suggesting that these samples possess the same boron chemical environment. Similarly, a single boron resonance at the chemical shift of −23 ppm was detected in the postmilled $Mg(NH_2BH_3)_2{\cdot}NH_3$ and KH sample (see Figure 3), which indicates a possible formation of the new species of $K_2Mg(NH_2BH_3)_4$. Furthermore, a slight downfield and upfield shift can be observed relative to those observed in pristine AB and $Mg(NH_2BH_3)_2{\cdot}NH_3$, respectively. This result suggests that a substantial change in the boron chemical environment occurs,

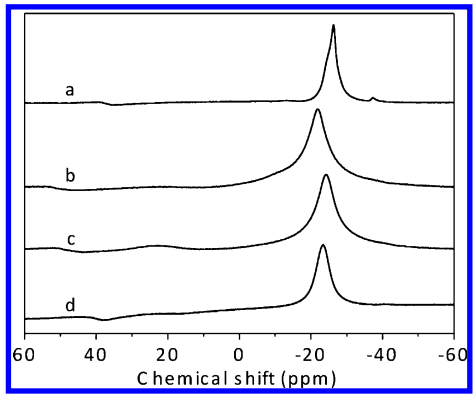

Figure 3. ^{11}B MAS NMR spectra of (a) AB, (b) $Mg(NH_2BH_3)_2{\cdot}NH_3$, (c) the postmilled $Mg(NH_2BH_3)_2{\cdot}NH_3$+NaH, and (d) $Mg(NH_2BH_3)_2{\cdot}NH_3$+KH.

dx.doi.org/10.1021/cm301662q | Chem. Mater. 2012, 24, 3574–3581

consistent with the observation of red and blue shifts in the B−H, N−H, and B−N vibrations in the IR spectra.

The XRD pattern of the postmilled $Mg(NH_2BH_3)_2{\cdot}NH_3$ and KH or $[K_2Mg(NH_2BH_3)_4+Mg(NH_2)_2]$ composite can be indexed by using tetragonal cell with the space group of $I4_1/a$. The lattice constants were determined as $a = b = 9.5974(17)$ Å, $c = 13.581(4)$ Å and $\alpha = \beta = \gamma = 90°$. The Rietveld fit of the XRD pattern and the detailed crystallographic information are included in the Supporting Information (see Figure S6). Figure 4 illustrates the relaxed structure of $K_2Mg(NH_2BH_3)_4$ and the

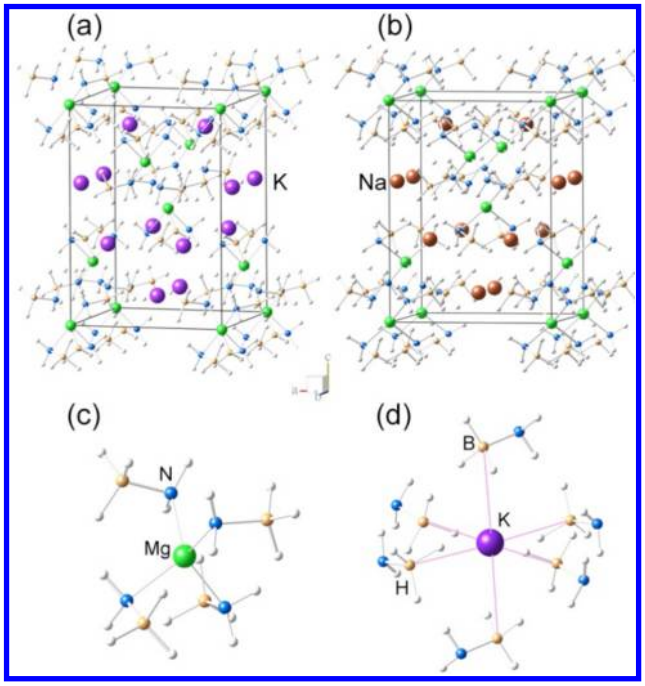

Figure 4. Molecular packing of (a) $K_2Mg(NH_2BH_3)_4$, (b) $Na_2Mg(NH_2BH_3)_4$, (c) coordination sphere surround by Mg^{2+}, and (d) coordination sphere surround by K^+.

close contacts around Mg^{2+} and K^+, respectively. A very unique coordination was observed, i.e., Mg^{2+} is tetrahedrally bound with N from four $(NH_2BH_3)^-$ anionic groups, forming $[Mg(NH_2BH_3)_4]^{2-}$ species (Figure 4C). The Mg−N bonds have an equal bond length of 2.115 Å, which is close to the Mg−N bond length observed in $Mg(NH_2BH_3)_2{\cdot}NH_3$ (2.104 and 2.129 Å)[26] and $Mg(NH_2)_2$ (1.997−2.172 Å).[41] Different from Mg^{2+}, K^+ is octahedrally coordinated with six $(NH_2BH_3)^-$ groups due to its relatively large ionic radius (Figure 4D). No direct K−N bond is formed, rather, six K···BH_3 coordinations are established with the K···B distances of 3.361, 3.431, and 3.617 Å, which are similar to that seen in KBH_4 (3.364 Å).[42] The charge borne by K^+ is balanced via K···H(BH_3) interaction (the BH_3 groups are of high electron density due to the anionic $[Mg(NH_2BH_3)_4]^{2-}$ species). $Na_2Mg(NH_2BH_3)_4$ is an isostructure of its analogue compound $K_2Mg(NH_2BH_3)_4$ (see Figure 4B).[12] Due to the similar configuration, the FTIR spectra of $[K_2Mg(NH_2BH_3)_4+Mg(NH_2)_2]$ and $[Na_2Mg(NH_2BH_3)_4+Mg(NH_2)_2]$ resemble each other fairly well (Figure 2). Similarly, such a kind of coordination was also observed in the crystal structure of the $NaLi(NH_2BH_3)_2$ where all the strong Lewis bases (NH_2) coordinate to a stronger Lewis acid (Li^+) and the weaker Lewis acid (Na^+) coordinates to the weaker Lewis bases (BH_3).[14]

To gain further insight in the hydrogen desorption properties of the $[K_2Mg(NH_2BH_3)_4+Mg(NH_2)_2]$ and $[Na_2Mg(NH_2BH_3)_4+Mg(NH_2)_2]$ composites, respectively, thermal decomposition of those samples were investigated by TG−DSC and TPD−MS (see Figure 5). Different from pristine

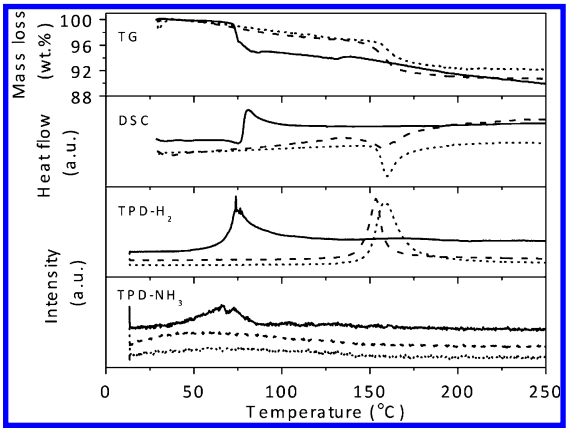

Figure 5. Comparison of the TG-DSC and TPD−MS curves of $Mg(NH_2BH_3)_2{\cdot}NH_3$ (solid line), $Na_2Mg(NH_2BH_3)_4+Mg(NH_2)_2$ (dashed line), and $K_2Mg(NH_2BH_3)_4+Mg(NH_2)_2$ (dotted line) composites. The temperature was ramped at 2 °C/min.

$Mg(NH_2BH_3)_2{\cdot}NH_3$, which NH_3 was coproduced with the release of H_2 at low temperatures, both composites released minor NH_3 prior to the dehydrogenation process in a wide temperature range beginning from ambient temperature to 150 °C. Based on the TG measurement, a weight loss of 3.7 wt.% and 3.8 wt.% were detected from $[K_2Mg(NH_2BH_3)_4+Mg(NH_2)_2]$ and $[Na_2Mg(NH_2BH_3)_4+Mg(NH_2)_2]$ composites, respectively, at temperatures <150 °C. Apparently, these weight losses are contributed to NH_3 release. Hydrogen, on the other hand, was released monotonically at temperatures above 147 or 141 °C, with a peak temperature of ca. 158 or 153 °C, respectively. It is worth highlighting that similar dehydrogenation behavior can also be seen in the pristine $Na_2Mg(NH_2BH_3)_4$, except that no significant NH_3 was detected at low temperatures (see Figure S7). In comparison to the thermal desorption of $Mg(NH_2BH_3)_2{\cdot}NH_3$ reported earlier which exhibits a broad hydrogen desorption profile covering a wide temperature range of 50−300 °C, the hydrogen desorption from the composite systems release hydrogen within a narrower temperature range. Matching with TG results, mass losses of ca. 4.4 wt.% and 5.8 wt.% of H_2 were released from $[K_2Mg(NH_2BH_3)_4+Mg(NH_2)_2]$ and $[Na_2Mg(NH_2BH_3)_4+Mg(NH_2)_2]$ composites, respectively. Most importantly, the hydrogen releases from all the samples are of endothermic nature as evidenced by TG-DSC measurements under open-system conditions, i.e., 5.2 kJ/mol H_2 (or 9.4 kJ/mol AB) for the $Na_2Mg(NH_2BH_3)_4+Mg(NH_2)_2$ and 7.0 kJ/mol H_2 (or 10.9 kJ/mol AB) for $K_2Mg(NH_2BH_3)_4+Mg(NH_2)_2$, respectively. C80 DSC measurements on the closed-system dehydrogenation also revealed an endothermic feature in the $K_2Mg(NH_2BH_3)_4+Mg(NH_2)_2$ composite. However, the reaction heat of the $Na_2Mg(NH_2BH_3)_4+Mg(NH_2)_2$ composite lies under the baseline which is statistically indistinguishable (see Figure S8). It is worth mentioning that there was no visual observation of melting phenomena in the heating process; therefore, the endothermic nature should be related to the dehydrogenation of the sample itself. It is obvious that a remarkable

dx.doi.org/10.1021/cm301662q | Chem. Mater. 2012, 24, 3574−3581

improvement in the dehydrogenation thermodynamics has been achieved via metal hydride alteration, tuning an exothermic hydrogen release (either from pristine AB or $Mg(NH_2BH_3)_2{\cdot}NH_3$) to an endothermic process.

The hydrogen storage capacities in $K_2Mg(NH_2BH_3)_4$+$Mg(NH_2)_2$ and $Na_2Mg(NH_2BH_3)_4$+$Mg(NH_2)_2$ were further quantified by volumetric release measurements, respectively. The results are shown in Figure 6. A total of ca. 7 and 7.8 wt %

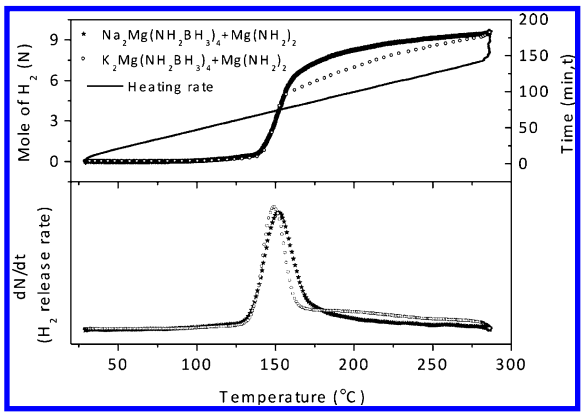

Figure 6. (Top) Volumetric release measurements on $Na_2Mg(NH_2BH_3)_4$+$Mg(NH_2)_2$, $K_2Mg(NH_2BH_3)_4$+$Mg(NH_2)_2$, and $Na_2Mg(NH_2BH_3)_4$ with a ramping rate of 2 °C/min to 285 °C. (Bottom) Differential results of hydrogen release.

which corresponds to 9.7 and 9.6 equiv of H_2 per $K_2Mg(NH_2BH_3)_4$+$Mg(NH_2)_2$ or $Na_2Mg(NH_2BH_3)_4$+$Mg(NH_2)_2$ were obtained upon raising temperature to 285 °C, respectively, with an accelerated H_2 release rate at ca. 150 °C. Compared to the H_2 weight losses measured via TG, more hydrogen was released in volumetric release measurement as a result of the participation of NH_3 in the dehydrogenation (closed-system). Upon dehydrogenation, only 0.6% and 1% of NH_3 can be detected in the gaseous phase, respectively. Unfortunately, XRD measurements of the dehydrogenated solid residues revealed the formation of amorphous phases. However, ^{11}B MAS NMR characterization of those samples (Figure 7) showed a boron resonance ranging from the chemical shift of 40 to 0 ppm, implying the presence of BN_2 or BN_3 species. In addition to the BN environment, a weak BH_4

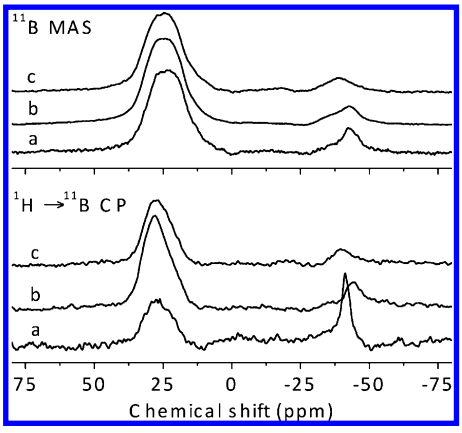

Figure 7. ^{11}B and $^1H \rightarrow {}^{11}B$ cross-polarization (CP) MAS NMR of postdehydrogenated samples at 300 °C of a) $Na_2Mg(NH_2BH_3)_4$, b) $Na_2Mg(NH_2BH_3)_2$+$Mg(NH_2)_2$, and c) $K_2Mg(NH_2BH_3)_4$+$Mg(NH_2)_2$.

resonance at the region of −39 to −42 ppm is observable in all the postdehydrogenated samples. On the other hand, the $^1H \rightarrow {}^{11}B$ cross-polarization experiment revealed the presence of H species bound to boron in B−N species, in addition to the boron in BH_4. Obviously, the ^{11}B resonances are parallel to that found in the postdehydrogenated $Na_2Mg(NH_2BH_3)_4$, suggesting that the remaining H in the residue may exist in the form of $Na_2Mg(NBH)_4$ or $K_2Mg(NBH)_4$ in the products together with the presence of BH_4 byproducts, consistent with the detection of B−H vibration in FTIR characterizations (Figure S9).

Because the dehydrogenation endothermicity of $K_2Mg(NH_2BH_3)_4$+$Mg(NH_2)_2$ and $Na_2Mg(NH_2BH_3)_4$+$Mg(NH_2)_2$ are too small to direct the dehydrogenation behavior, the dehydrogenation temperature is thus expected to be dominantly attributed to the kinetic barrier. It is also worth underlining that in the presence of Si as dispersant, more than 20 °C reduction in the dehydrogenation temperature was achieved in the $K_2Mg(NH_2BH_3)_4$+$Mg(NH_2)_2$ sample (Figure S10). Although the exact mechanism of Si is pending for further study, the existence of kinetic barrier during the hydrogen release is obvious. Therefore, the Kissinger method was adopted to determine the activation energies involved in the dehydrogenation of $Na_2Mg(NH_2BH_3)_4$+$Mg(NH_2)_2$ and $K_2Mg(NH_2BH_3)_4$+$Mg(NH_2)_2$ composites, respectively. The temperature at which the dehydrogenation rate is at its maximum (T_m) was identified by using TPD measurement. The TPD profiles of the hydrogen release at different heating rates were summarized in Figure S11. Based on the Kissinger's plot (Figure S12), the activation energies, E_a, for the hydrogen release is about 111 and 116 kJ/mol for the two composites, respectively. It is worth mentioning that the activation energy of pristine $Na_2Mg(NH_2BH_3)_4$ was determined to be 113 kJ/mol, which is close to the composite systems. This result suggests that metal hydride mediation may be the internal barrier that dominates the kinetic barrier of the composite systems, and those composites are kinetically stable.

$K_2Mg(NH_2BH_3)_4$ or $Na_2Mg(NH_2BH_3)_4$ rather than the hypothetic $Mg(NH_2BH_3)_2$ was detected in the interaction of $Mg(NH_2BH_3)_2{\cdot}NH_3$ and KH or NaH. From the thermodynamic stability point of view, bimetallic amidoborane is more stable than monometallic amidoborane. In order to understand the thermodynamic change that ensues behind bimetallic amidoborane, we incorporated first-principles calculations to evaluate the thermodynamic properties of $Na_2Mg(NH_2BH_3)_4$ and $K_2Mg(NH_2BH_3)_4$ and compared them to $NaNH_2BH_3$, KNH_2BH_3, and AB. As shown in Figure S13 and the calculated enthalpy of AB agrees well with the experimental data, showing that the harmonic approximation provides a good description of the thermodynamics of NH_3BH_3, and therefore it is feasible to be used to describe the thermodynamic properties of $NaNH_2BH_3$, $Na_2Mg(NH_2BH_3)_4$, KNH_2BH_3, and $K_2Mg(NH_2BH_3)_4$ (see Figure S14). As can be seen in Figure 8, the formation enthalpy at the same temperatures decreases from AB to $NaNH_2BH_3$ and $Na_2Mg(NH_2BH_3)_4$ to KNH_2BH_3 and $K_2Mg(NH_2BH_3)_4$. This result suggests that the stability of AB increases as a result of the substitution of one protonic H with an electropositive metal cation, which may be due to the stabilization effect of the ionic bond between M^{n+} and $[NH_2BH_3]^-$. The stability of $M(NH_2BH_3)_n$ appears to be related to the Pauling electronegativity, χ_p of the M. The stability increases with decreasing χ_p of the M (0.98 for Li, 0.93 for Na and 0.82 for K) indicating a higher charge transfer from M^{n+} to $[NH_2BH_3]^-$ to form a stronger ionic bond. This

dx.doi.org/10.1021/cm301662q | Chem. Mater. 2012, 24, 3574−3581

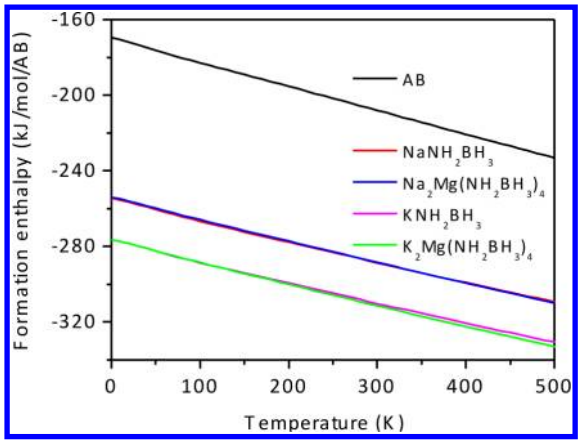

Figure 8. The temperature dependences of formation enthalpies (ΔH, in the unit of kJ/mol/AB) of solid NH_3BH_3, $NaNH_2BH_3$, $Na_2Mg(NH_2BH_3)_4$, KNH_2BH_3, and $K_2Mg(NH_2BH_3)_4$.

observation agrees with those reported by Nakamori et al. for $M(BH_4)_n$, which suggests Pauling electronegativity, χ_p as an indicator to estimate the stability of $M(BH_4)_n$.[43] Although there is no direct ionic bonding observed between Na or K and $[NH_2BH_3]^-$ in the bimetallic amidoboranes (see Figure 3d), the influences of electronegativity of Na and K may remain toward the $Mg(NH_2BH_3)_4^{2-}$ anion via Na···H and K···H coordinations.

In this study, we also proposed a reactant stabilization approach in tuning the thermodynamic properties of amidoboranes. To better visualize the stabilizing effect, Figure 9 is drawn based on the thermodynamic data available (both

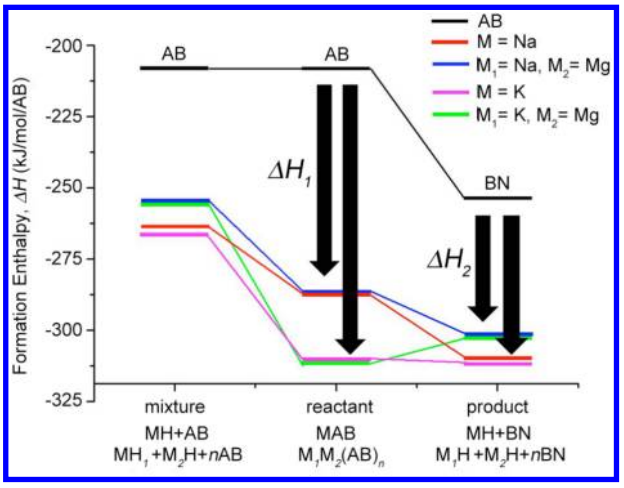

Figure 9. Reduction of dehydrogenation exothermicity via reactant stabilization approach.

theoretical and experimental). As reported previously, $NaNH_2BH_3$ decomposes to release H_2 and form NaH and BN.[44] Recently, Kojima and co-workers employed solid state NMR to quantitatively study the decomposition of $NaNH_2BH_3$ and reported that $Na_{0.5}NBH_{0.5}$ (or a mixture of *h*−BN and NaNBH-like structure) and NaH were detected in the decomposition residue.[45] We ball milled NaH and BN under ambient conditions for 24 h at 200 rpm but still can observe the individual components indicating that NaNBH may be a "metastable" phase formed in the dehydrogenation, in which NaH encounters a relatively high barrier to be separated from BN. Therefore, an assumption is made for the ease of illustration, that is, by assuming that metal amidoborane (MAB) and bimetallic amidoborane ($M_1M_2AB_n$) decompose to form corresponding metal hydrides (MH) and boron nitride (BN). As can be seen in Figure 9, reacting AB with metal hydrides results in a significant decrease in the formation enthalpy of the reactants, i.e., formation of more stable compound with large value of ΔH_1. ΔH_1, herein, can be defined as the enthalpy change that corresponds to the stabilization process, which is considerably larger than the enthalpy change observed in the product (ΔH_2) resulting from product stabilization by metal cation. Obviously, metal hydride has a more dominant stabilizing effect toward the reactants than the products. Based on Figure 9, dehydrogenation of $Na_2Mg(NH_2BH_3)_4$ is an exothermic process to give 2NaH +MgH_2+4BN. However, an endothermic dehydrogenation from $Na_2Mg(NH_2BH_3)_4$ was observed in our experimental results (see Figure S7). This difference may be due to the overestimation of thermodynamic stability of the compounds formed after the dehydrogenation process. In the composite systems where $Mg(NH_2)_2$ exists, the endothermic dehydrogenation may also be attributed by the interaction of bimetallic amidoborane and $Mg(NH_2)_2$, forming less stable solid residue compared to the starting composites. Despite much information on the functional groups could be deduced from spectroscopic data, still there is insufficient evidence for an unambiguous claim on the possible species present in the dehydrogenation residue. In view of the thermodynamic improvement, forming a stable reactant appears to be an effective way of reducing the exothermicity of the dehydrogenation of amidoborane. In contrary, to reduce the endothermicity of a reversible dehydrogenation process, reactant destabilization is to be employed. To date, only a few metal amidoboranes were reported to release hydrogen endothermically. Burrell and co-workers reported an estimation of dehydrogenation enthalpy of 3.5 kJ/mol from $Ca(NH_2BH_3)_2$.[6] The bimetallic amidoborane, $NaMg(NH_2BH_3)_3$, which is of different composition from $Na_2Mg(NH_2BH_3)_4$ reported by Wu et al.,[12] was reported to dehydrogenate endothermically with a reaction enthalpy of ca. 3.4 kJ/mol by Wang et al.[13]

In addition to the stabilization approach discussed earlier, it is worthwhile to investigate the strength differences in the chemical bonds of $NaNH_2BH_3$, KNH_2BH_3, $Na_2Mg(NH_2BH_3)_4$, and $K_2Mg(NH_2BH_3)_4$, given that the reaction enthalpy reflects the sum of the energy involve in the bond breaking (endothermic) and bond formation (exothermic). To have an

Table 1. Calculated Interatomic Distances (Å) in $NaNH_2BH_3$, KNH_2BH_3, $Na_2Mg(NH_2BH_3)_4$, and $K_2Mg(NH_2BH_3)_4$

	B−N	B−H	N−H	Na···H	Mg−N	Na−N	K···H	K−N
$NaNH_2BH_3$	1.544	1.238−1.255	1.022	2.310−2.391	–	2.378	–	–
$Na_2Mg(NH_2BH_3)_4$	1.570	1.232−1.238	1.026	2.326	2.098	–	–	–
KNH_2BH_3	1.546	1.238−1.256	1.024	–	–	–	2.630−2.950	2.970−3.194
$K_2Mg(NH_2BH_3)_4$	1.575	1.235	1.026	–	2.100	–	2.606−3.093	–

dx.doi.org/10.1021/cm301662q | *Chem. Mater.* 2012, 24, 3574−3581

overview on the variation in the bond strength, we compare the structural information, FTIR spectra, and phonon density of states (PDOS) of $NaNH_2BH_3$, KNH_2BH_3, $Na_2Mg(NH_2BH_3)_4$, and $K_2Mg(NH_2BH_3)_4$, and the results are presented in Table 1 and Figure S15−20. Calculated structures were used to allow direct comparison. As shown in Table 1, B−N, N−H, and the shortest Na···H coordination are longer, while B−H is shorter in $Na_2Mg(NH_2BH_3)_4$ than those in $NaNH_2BH_3$. Similar variation in the bond distances can also be observed in the case of $K_2Mg(NH_2BH_3)_4$ and KNH_2BH_3 except for the K···H coordination. These variations agree fairly well with the red shifts of B−N, N−H and the blue shift of B−H bands in FTIR and PDOS of $NaNH_2BH_3$ and $Na_2Mg(NH_2BH_3)_4$, KNH_2BH_3 and $K_2Mg(NH_2BH_3)_4$ (FTIR spectra of KNH_2BH_3 is not available), respectively. Structural analyses of $Na_2Mg(NH_2BH_3)_4$ and $K_2Mg(NH_2BH_3)_4$ show that Na^+ and K^+ cations are octahedrally surrounded by six BH_3 groups of $[NH_2BH_3]^-$ and are stabilized only via Na(K)···H coordination. Therefore, it is likely that a metal hydride mediated dehydrogenation would occur in $Na_2Mg(NH_2BH_3)_4$ and $K_2Mg(NH_2BH_3)_4$. Based on the metal hydride mediated pathway proposed by Kim et al.[15,17] and Lee et al.,[16] the hydridic H^- may be transferred from BH_3 to Na or K, forming Na−H or K−H, and subsequently, the Na−H may interact with protonic H^+ in the $Mg(NH_2BH_3)_4^{2-}$ group to release H_2, forming B−N bond concomitantly. Due to the fact that the formation of metal hydride (Na−H or K−H in this case) involves rate-limiting step, the strengthened B−H bonds and some weakened Na(K)···H in $Na_2Mg(NH_2BH_3)_4$ or $K_2Mg(NH_2BH_3)_4$ reflect an increase in dehydrogenation temperature compared to $NaNH_2BH_3$ or KNH_2BH_3. In the case of the composite system, there may exist competition between the $Mg(NH_2BH_3)_4^{2-}$ group and $Mg(NH_2)_2$ to react with Na−H or K−H to release H_2. It is worthy of highlighting that the dehydrogenation of bimetallic amidoborane (or the composite) is likely an interaction of NaH with $Mg(NH_2)_2$, which is a reversible hydrogen storage system with the dehydrogenation enthalpy of ca. 79 kJ/mol−H_2.[46] It releases H_2 at a peak temperature of ca. 160 °C. Not being forgotten, concordant formation of B−N or B=N bond occurs in the dehydrogenation of these bimetallic amidoboranes, and the bond formation is an energy decreasing process (exothermic). Thus, the mild endothermicity of $Na_2Mg(NH_2BH_3)_4$ may be a result of an averaging effect of the endothermic H_2 release and exothermic B−N bond formation processes. This may also be true for $K_2Mg(NH_2BH_3)_4$ whereby the interaction of KH with $Mg(NH_2)_2$ releases H_2 reversibly in a stepwise manner in temperature range of 120−225 °C with ΔH = 56 kJ/mol−H_2.[47]

CONCLUSION

In this study, thermodynamic alteration of $Mg(NH_2BH_3)_2{\cdot}NH_3$ has been achieved by addition of NaH or KH, forming a composite that is composed of bimetallic amidoborane and magnesium amide. The crystal structure of $K_2Mg(NH_2BH_3)_4$ and $Na_2Mg(NH_2BH_3)_4$ were identified and solved by X-ray powder diffraction. The hydrogen storage properties of these composites were investigated, and the thermodynamic data of pristine bimetallic amidoboranes were obtained by first-principles calculations. $[K_2Mg(NH_2BH_3)_4+Mg(NH_2)_2]$ and $[Na_2Mg(NH_2BH_3)_4+Mg(NH_2)_2]$ composites were found to dehydrogenate 7 wt.% and 7.8 wt.% of H_2 endothermically upon heated to 285 °C, respectively.

Although the role of $Mg(NH_2)_2$ in inducing endothermic dehydrogenation with bimetallic amidoborane remains uncertain, the discovery of endothermic dehydrogenation in bimetallic amidoborane and the inimitable role plays by metal cations in increasing the stability of the amidoborane provide insights for further development of bimetallic amidoboranes with different thermodynamic stability. Coupling with off-board regeneration, this thermodynamic favorable dehydrogenation process makes bimetallic amidoborane a potential material for hydrogen storage. Designing new bimetallic amidoborane by matching metal cation pairs with different Pauling electronegativities to achieve a more thermodynamic stable reactant is thus worth a detail research. Further in-depth investigation on the interaction between bimetallic amidoborane and amide is also needed. Catalyst addition may be a subject for future research to improve the hydrogen release kinetic barrier. Theoretical study on the dehydrogenation mechanism of these systems is important as it may shine a light toward better understanding on the significant thermodynamic improvement in the hydrogen release.

ASSOCIATED CONTENT

Supporting Information

cif of $K_2Mg(NH_2BH_3)_4$ and $Na_2Mg(NH_2BH_3)_4$, experimental procedure, C80 characterization, XRD patterns, Rietveld fit of the XRD patterns, FTIR, TPD−MS, Kissinger plot, FTIR spectra, calculated phonon density of states and calculated enthalpy of various metal amidoboranes. This material is available free of charge via the Internet at http://pubs.acs.org.

AUTHOR INFORMATION

Corresponding Author

*E-mail: pchen@dicp.ac.cn.

Notes

The authors declare no competing financial interest.

ACKNOWLEDGMENTS

The authors acknowledge financial support from Hundred Talents Project and Knowledge Innovation Program of CAS (KJCX2-YW-H21), 973 Project (2010CB631304), and the National Natural Science Foundation of China (no. 10979051, 20971120, and 20973162). Y.S.C. would like to thank Hui Wu for helpful discussions and advice on structural refinement.

REFERENCES

(1) Stephens, F. H.; Pons, V.; Baker, R. T. *Dalton Trans.* **2007**, 2613.
(2) Staubitz, A.; Robertson, A. P. M.; Manners, I. *Chem. Rev.* **2010**, *110*, 4079.
(3) Chua, Y. S.; Chen, P.; Wu, G.; Xiong, Z. *Chem. Commun.* **2011**, *47*, 5116.
(4) Gutowska, A.; Li, L.; Shin, Y.; Wang, C. M.; Li, X. S.; Linehan, J. C.; Smith, R. S.; Kay, B. D.; Schmid, B.; Shaw, W.; Gutowski, M.; Autrey, T. *Angew. Chem., Int. Ed.* **2005**, *44*, 3578.
(5) Xiong, Z. T.; Yong, C. K.; Wu, G. T.; Chen, P.; Shaw, W.; Karkamkar, A.; Autrey, T.; Jones, M. O.; Johnson, S. R.; Edwards, P. P.; David, W. I. F. *Nat. Mater.* **2008**, *7*, 138.
(6) Diyabalanage, H. V. K.; Shrestha, R. P.; Semelsberger, T. A.; Scott, B. L.; Bowden, M. E.; Davis, B. L.; Burrell, A. K. *Angew. Chem., Int. Ed.* **2007**, *46*, 8995.
(7) Kang, X. D.; Fang, Z. Z.; Kong, L. Y.; Cheng, H. M.; Yao, X. D.; Lu, G. Q.; Wang, P. *Adv. Mater.* **2008**, *20*, 2756.
(8) Wu, H.; Zhou, W.; Yildirim, T. *J. Am. Chem. Soc.* **2008**, *130*, 14834.

(9) Diyabalanage, H. V. K.; Nakagawa, T.; Shrestha, R. P.; Semelsberger, T. A.; Davis, B. L.; Scott, B. L.; Burrell, A. K.; David, W. I. F.; Ryan, K. R.; Jones, M. O.; Edwards, P. P. *J. Am. Chem. Soc.* **2010**, *132*, 11836.
(10) Genova, R. V.; Fijalkowski, K. J.; Budzianowski, A.; Grochala, W. *J. Alloys Compd.* **2010**, *499*, 144.
(11) Zhang, Q. G.; Tang, C. X.; Fang, C. H.; Fang, F.; Sun, D.; Ouyang, L. Z.; Zhu, M. *J. Phys. Chem. C* **2010**, *114*, 1709.
(12) Wu, H.; Zhou, W.; Pinkerton, F. E.; Meyer, M. S.; Yao, Q.; Gadipelli, S.; Udovic, T. J.; Yildirim, T.; Rush, J. J. *Chem. Commun.* **2011**, *47*, 4102.
(13) Kang, X.; Luo, J.; Zhang, Q.; Wang, P. *Dalton Trans.* **2011**, *40*, 3799.
(14) Fijalkowski, K. J.; Genova, R. V.; Filinchuk, Y.; Budzianowski, A.; Derzsi, M.; Jaroń, T.; Leszczyński, P. J.; Grochala, W. *Dalton Trans.* **2011**, *40*, 4407.
(15) Kim, D. Y.; Singh, N. J.; Lee, H. M.; Kim, K. S. *Chem.–Eur. J.* **2009**, *15*, 5598.
(16) Lee, T. B.; McKee, M. L. *Inorg. Chem.* **2009**, *48*, 7564.
(17) Kim, D. Y.; Lee, H. M.; Seo, J.; Shin, S. K.; Kim, K. S. *Phys. Chem. Chem. Phys.* **2010**, *12*, 5446.
(18) Luedtke, A. T.; Autrey, T. *Inorg. Chem.* **2010**, *49*, 3905.
(19) Spielmann, J.; Jansen, G.; Bandmann, H.; Harder, S. *Angew. Chem., Int. Ed.* **2008**, *47*, 6290.
(20) Spielmann, J.; Piesik, D. F. J.; Harder, S. *Chem.–Eur. J.* **2010**, *16*, 8307.
(21) Spielmann, J.; Harder, S. *J. Am. Chem. Soc.* **2009**, *131*, 5064.
(22) Spielmann, J.; Harder, S. *Dalton Trans.* **2011**, *40*, 8314.
(23) Chua, Y. S.; Wu, G. T.; Xiong, Z. T.; He, T.; Chen, P. *Chem. Mater.* **2009**, *21*, 4899.
(24) Xia, G. L.; Yu, X. B.; Guo, Y. H.; Wu, Z.; Yang, C. Z.; Liu, H. K.; Dou, S. X. *Chem.–Eur. J.* **2010**, *16*, 3763.
(25) Graham, K. R.; Kemmitt, T.; Bowden, M. E. *Energy Environ. Sci.* **2009**, *2*, 706.
(26) Chua, Y. S.; Wu, G. T.; Xiong, Z. T.; Karkamkar, A.; Guo, J. P.; Jian, M. X.; Wong, M. W.; Autrey, T.; Chen, P. *Chem. Commun.* **2010**, *46*, 5752.
(27) Chua, Y. S.; Li, W.; Shaw, W. J.; Wu, G.; Autrey, T.; Xiong, Z.; Wong, M. W.; Chen, P. *ChemSusChem* **2012**, *5*, 927.
(28) Li, W.; Wu, G.; Chua, Y.; Feng, Y. P.; Chen, P. *Inorg. Chem.* **2011**, *51*, 76.
(29) Bhattacharya, S.; Xiong, Z.; Wu, G.; Chen, P.; Feng, Y. P.; Majumder, C.; Das, G. P. *J. Phys. Chem. C* **2012**, *116*, 8859.
(30) Harder, S.; Spielmann, J.; Tobey, B. *Chem.–Eur. J.* **2012**, *18*, 1984.
(31) Hu, Y. H.; Ruckenstein, E. *J. Phys. Chem. A* **2003**, *107*, 9737.
(32) Chen, P.; Xiong, Z. T.; Luo, J. Z.; Lin, J. Y.; Tan, K. L. *J. Phys. Chem. B* **2003**, *107*, 10967.
(33) Larson, A. C.; Von Dreele, R. B. *General Structure Analysis System (GSAS)*; Report LAUR 86-748; Los Alamos National Laboratory: 2004.
(34) Kresse, G.; Joubert, D. *Phys. Rev. B* **1999**, *59*, 1758.
(35) Kresse, G.; Hafner, J. *Phys. Rev. B* **1993**, *47*, 558.
(36) Kresse, G.; Furthmuller, J. *Comput. Mater. Sci.* **1996**, *6*, 15.
(37) Kresse, G.; et al. *EPL (Europhys. Lett.)* **1995**, *32*, 729.
(38) Parlinski, K.; Li, Z. Q.; Kawazoe, Y. *Phys. Rev. Lett.* **1997**, *78*, 4063.
(39) Togo, A. Phonopy Program. http://phonopy.sourceforge.net/ (accessed March 2011).
(40) Hu, J.; Wu, G.; Liu, Y.; Xiong, Z.; Chen, P.; Murata, K.; Sakata, K.; Wolf, G. *J. Phys. Chem. B* **2006**, *110*, 14688.
(41) Sorby, M.; Nakamura, Y.; Brinks, H.; Ichikawa, T.; Hino, S.; Fujii, H.; Hauback, B. *J. Alloys Compd.* **2007**, *428*, 297.
(42) Renaudin, G.; Gomes, S.; Hagemann, H.; Keller, L.; Yvon, K. *J. Alloys Compd.* **2004**, *375*, 98.
(43) Nakamori, Y.; Miwa, K.; Ninomiya, A.; Li, H.; Ohba, N.; Towata, S.-i.; Züttel, A.; Orimo, S.-i. *Phys. Rev. B* **2006**, 74.
(44) Xiong, Z. T.; Wu, G. T.; Chua, Y. S.; Hu, J. J.; He, T.; Xu, W. L.; Chen, P. *Energy Environ. Sci.* **2008**, *1*, 360.
(45) Shimoda, K.; Zhang, Y.; Ichikawa, T.; Miyaoka, H.; Kojima, Y. *J. Mater. Chem.* **2011**, *21*, 2609.
(46) Xiong, Z. T.; Hu, J. J.; Wu, G. T.; Chen, P. *J. Alloys Compd.* **2005**, *395*, 209.
(47) Wang, J.; Wu, G.; Chua, Y. S.; Guo, J.; Xiong, Z.; Zhang, Y.; Gao, M.; Pan, H.; Chen, P. *ChemSusChem* **2011**, *4*, 1622.